https://doi.org/10.5194/egusphere-2024-1257
Preprint. Discussion started: 6 May 2024

Dynamic and thermodynamic contribution to the October 2019 exceptional rainfall in West Central Africa

Kevin Kenfack[1*] · **Francesco Marra**[3] · **Zéphirin Yepdo Djomou**[1,2] · **Lucie A. Djiotang Tchotchou**[1] · **Alain T. Tamoffo**[4] · **Derbetini A. Vondou**[1]

[1]Laboratory for Environmental Modelling and Atmospheric Physics (LEMAP), Physics Department, University of Yaoundé 1, Yaoundé, Cameroon

[2]National Institute of Cartography, Cameroon

[3]Department of Geosciences, University of Padova, Italy

[4]Climate Service Center Germany (GERICS), Helmholtz-Zentrum Hereon, Fischertwiete 1, 20095 Hamburg, Germany

Corresponding author: **Kevin Kenfack**

Email: **kevinkenfack46@gmail.com**

ORCID: **0000-0003-1694-4906**

Kevin Kenfack’s ORCID: 0000-0003-1694-4906

Francesco Marra’s ORCID: 0000-0003-0573-9202

Lucie A. Djiotang Tchotchou’s ORCID: 0000-0003-2860-428X

Alain T. Tamoffo’s ORCID: 0000-0001-8482-8881

Derbetini A. Vondou’s ORCID: 0000-0002-8681-5328

https://doi.org/10.5194/egusphere-2024-1257
Preprint. Discussion started: 6 May 2024

Abstract

Exceptional rainfall hit West Central Africa in October 2019. To understand the underlying mechanisms, we diagnosed the regional moisture and Moist Static Energy (MSE) budgets with a view to highlighting the importance of the dynamic and thermodynamic effects associated with this historic event. Analysis of the moisture budget reveals that the precipitation anomalies in October were mainly controlled by dynamic effects (72.5% of the sum of dynamic and thermodynamic contributions). Horizontal moisture advection induced by horizontal wind anomalies controls extreme precipitation north of West Central Africa, while vertical moisture advection induced by vertical velocity anomalies controls extreme precipitation south of West Central Africa. Changes in the thermodynamic effect, although not the key factor responsible for the events of October 2019, contribute up to 27.5% of the total effect. Diagnosis of the MSE balance shows that the anomalous vertical motion is dominated by the dynamic effect, i.e. the wet enthalpy advection induced by the horizontal wind anomalies. The horizontal advection of the MSE induced by the variation of the wet enthalpy and the vertical advection of the MSE induced by the variation of the MSE seem less important. The variations in the MSE balance are linked to its meridional component, in particular the meridional wind anomalies in the dynamic effect and the meridional variations in latent heat in the thermodynamic effect. This is due to the increase in sea surface temperatures in the equatorial Atlantic, associated with the anomalous thermal depression over the Sahara, which has increased rainfall over West Central Africa. Our results suggest that dynamic and thermodynamic effects should be jointly considered for adequately anticipating this kind of extreme event. Understanding the associated mechanisms could help us improve our projections and increase the region's population resilience to these extreme weather events.

Keywords: West Central Africa · Moisture budget · Moist static energy budget · Precipitation · wet enthalpy

https://doi.org/10.5194/egusphere-2024-1257
Preprint. Discussion started: 6 May 2024

1 Introduction

Equatorial Africa recorded unprecedented amounts of rainfall in October and November 2019 (Wainwright et al, 2020). Such a significant amount of precipitation is not without consequences for the population and the environment. In October, in most parts of East Africa in general, and in Kenya in particular, extreme rainfall led to flooding and landslides, provoking major destruction, with more than 100 deaths and around 18,000 people displaced internally and to neighboring countries (http://floodlist.com/africa/kenya-floods-november-2019). In Central Africa, the Democratic Republic of Congo has been devastated by major flooding and forestry disruption along the Congo River, forcing many people to move (Gou et al. 2022). In the Central African Republic, extreme and persistent rainfall caused significant flooding and landslides, including the Oubangui River overflowing nearly 60 km of its coastline (Igri et al. 2023). In addition, the night of 27 to 28 October 2019 was disastrous in the West Cameroon region, mainly in the locality of Bafoussam where extreme rainfall for about 36 hours caused a landslide, resulting in significant material damage with 45 dead and others missing (Aretouyap et al. 2021; Mfondoum et al. 2021; Wantim et al. 2023). The episode was associated with a thermal depression over the Sahara and with anomalously high Sea Surface Temperatures (SST). The occurrence of these conditions may change in response to anthropogenic global warming, raising the question whether devastating events such as the one of October 2019 could occur more frequently in the future (Nicholson et al. 2022). In particular, given that climate models predict an increasing trend in extreme rainfall in the region (Fotso-Nguemo et al. 2018, 2019; Sonkoué et al. 2018; Tamoffo et al. 2019, 2023) and that extreme precipitation in the region is associated with vegetation dynamics (Zhou et al. 2014; Mariotti et al. 2014; Marra et al. 2022; Garcin et al. 2018), it is crucial to understand the thermodynamic and dynamic mechanisms underlying these exceptional events

Recent studies have attempted to investigate the causes of extreme rainfall during the exceptional period of October 2019 in Equatorial Africa. Nicholson et al. (2022) showed that heavy rainfall on the Guinea coast was enhanced by positive sea surface temperature anomalies along the Atlantic coast. On the other hand, a significant increase in the flux of moisture originating in the Atlantic, combined with the convergence of humidity, is another important factor contributing to the increase in precipitation in the region (Pokam et al. 2011, Kuete et al. 2019). Wainwright et al. (2020) pointed out that the increase in rainfall over East Africa was a consequence of the positive phase of the Indian Ocean Dipole. Indeed, Black et al. (2005) reported that during periods of the year when the dipole mode index (DMI) IOD events are greater than 0.5°C over a period of 3 consecutive months and when the zonal SST gradient is reversed over several months, the resulting increase in rainfall over

https://doi.org/10.5194/egusphere-2024-1257
Preprint. Discussion started: 6 May 2024

East Africa is important. In addition, the positive IOD event of 2019 lasted from late summer through to December, influencing rainfall over East Africa.

Rainfall variability in Central Africa is highly dependent on the convergence of atmospheric moisture (Pokam et al. 2012; Washington et al., 2013; Dyer et al., 2017; Hua et al., 2019; Taguela et al. 2022). Under the effect of global warming, the increase in extreme precipitation is a consequence of the increase in available atmospheric humidity (Nicholson et al 2022). Although previous studies have focused on analyzing meteorological factors, there is still a general lack of knowledge about quantifying the dynamic and thermodynamic effects associated with these extremes of precipitation. In recent years, the decomposition of the water balance behind precipitation anomalies is often used to isolate the dynamic and thermodynamic contributions to extreme events (Li et al., 2017; Oueslati et al., 2019; Wen et al., 2022; Kenfack et al., 2023,2024). Water balance analysis has proved to be a useful tool for understanding anomaly fields in mean precipitation under the influence of global warming (Seager et al. 2014). Moist static energy (MSE), in particular, is a useful parameter for investigating the contribution of atmospheric moisture and analyzing vertical velocity (Wang and Li, 2020a, 2020b; Bell et a. 2015; Neelin, 2021; Nana et al. 2023; Andrews et al. 2023; Longandjo and Raoul, 2024; Kenfack et al. 2024). Recently, Kenfack et al. (2024) showed that, in the Congo Basin, the structure of the horizontal moisture advection anomalies is similar to that of the MSE advection anomalies during rainy seasons March-April-May (MAM) and September-October-November (SON). In addition, the atmospheric heating source has been identified as an indicator of precipitation (He et al. 2021). The increase in diabatic heating on the coast can contribute to the acceleration of near-surface winds (Pokam et al. 2014). An increase in this quantity implies an increase in latent warming which can induce the greenhouse effect and reinforce the moisture convergence, with a positive feedback process that leads to extreme precipitation. Further, it has been demonstrated that reducing the source of heating in recent decades has also led to a pronounced reduction in rainfall in reanalyses over the Congo Basin (Kenfack et al. 2024). Given the highlighted importance of moisture, MSE and heating sources on rainfall variability, we adopt in this study an approach based on diabatic heating, water balance and MSE to diagnose dynamic and thermodynamic processes associated with the October 2019 rainfall extremes over West Equatorial Africa.

The remainder of the paper is structured as follows. A description of the observation and reanalysis data, and analysis methods is presented in Section 2. Section 3 describes the diabatic heating source and the performance of the reanalysis in capturing the October 2019 precipitation extremes. In Section 4, we investigate the dynamic and thermodynamic effects associated with the moisture balance. The analysis of the dynamic and thermodynamic effects associated with the MSE

https://doi.org/10.5194/egusphere-2024-1257
Preprint. Discussion started: 6 May 2024

budget during the October 2019 rainfall anomaly period over West Central Africa is presented in Section 5. Section 6 is conclusions and discussions.

2 Data and methods

2.1. Data

In this study, datasets from the fifth version of the European Centre for Medium-Range Weather Forecasts reanalysis, known as ERA5 (Hersbach et al., 2020), are used for the analyses. Johannsen et al. (2019) established that over equatorial Africa, ERA5 significantly improves over ERA-Interim (which represents the previous dataset), particularly in the description of the hydrological cycle. In addition, Cook and Vizy (2021) have shown that ERA5 represents well the spatial distribution of precipitation and atmospheric dynamic fields compared with previous generations, particularly over the Congo Basin. With a spatial resolution of 0.25°×0.25°, ERA5 is a global reanalysis dataset available from 1979 to the present, covering 137 pressure levels from the surface to 0.01 hPa. Monthly variables including horizontal and vertical wind components, geopotential, evaporation, humidity, heat flux and temperature are used in this study. For all variables, anomalies are obtained by removing the 30-year mean of the period 1988 to 2017. To assess ERA5's ability to detect October 2019 precipitation extremes, we used three observational datasets, including rain gauge products and gauge-adjusted satellite products: the Climate Hazards Group InfraRed Precipitation with Stations (CHIRPS) gridded dataset, available at a resolution of 0.05° × 0.05° (Funk et al., 2015); the Global Precipitation Climatology Project (GPCP-v2.2) with a grid spacing of 2.5° × 2.5° (Huffman et al., 2009); the Climatic Research Unit (CRU-TS4.03) gridded data at a resolution of 0.5° × 0.5° (Harris et al., 2020).

2.2 Methods

2.2.1 Diabetic heating

Diabatic heating as proposed by Yanai and Tomita (1998) and Pokam et al. (2014) is defined as follows:

$$Q = \chi\left(\frac{\partial \theta}{\partial t} + u\frac{\partial \theta}{\partial x} + v\frac{\partial \theta}{\partial y} + \omega\frac{\partial \theta}{\partial p}\right) \quad (1)$$

$$\chi = c_p\left(\frac{T}{\theta}\right) \quad (2)$$

https://doi.org/10.5194/egusphere-2024-1257
Preprint. Discussion started: 6 May 2024

In equations 1 and 2, C_p (1,005 J Kg^{-1} K^{-1}) denotes the specific heat at constant pressure, θ is the potential temperature, ω is the vertical velocity (hPa s^{-1}), and$V=(u, v)$ is the vector of horizontal velocities. T (K) and p (hPa) represent the air temperature and the barometric pressure, respectively.

To quantify the monthly mean heating rate $\tau(K\, day^{-1})$ related to apparent heating, we use the relation:

$$\tau = (\frac{Q}{c_p}) \times 86400 \quad (3)$$

where Q is the combination of heat from radiation, latent heat from condensation and the convergence of vertical vortical transport of sensible heat.

2.2.2 Diagnosis of the moisture budget

The moisture budget used to quantify the contributions of evaporation and the horizontal and vertical components associated with the circulation of moist air in the atmosphere (Seager et al., 2010; Oueslati et al., 2019; Jiang et al., 2020; Moon and Ha, 2020; Wen et al., 2022; Zhao et al., 2022; Sheng et al., 2023; Kenfack et al., 2024) is defined as follows:

$$\langle \partial_t q \rangle + \langle V \cdot \nabla_h q \rangle + \langle \omega \cdot \partial_p q \rangle = E - P \quad (4)$$

In Eq. 4, q represents the specific humidity, $V=(u,v)$ denotes the horizontal wind and ω the vertical pressure velocity. E denotes surface evaporation and P precipitation. Angle brackets "⟨⟩" signify the mass integral from the surface (ps = 1000 hPa) to a pressure pt = 300 hPa which, as specified by Seager et al. (2010), represents the top of the atmosphere. The first term on the left of equation 4 can be neglected because q varies little over time on a monthly scale. To estimate the horizontal and vertical moisture advection components, we decompose equation 4 into its different linear and residual terms as follows:

$$P' = E' - \langle \bar{V} \cdot \nabla q' \rangle - \langle V' \cdot \nabla \bar{q} \rangle - \langle \bar{\omega} \partial_p q' \rangle - \langle \omega' \partial_p \bar{q} \rangle + Res \quad (5)$$

In Eq. 5, the overbar indicates the monthly mean climatology from 1988 to 2017 and primes indicate deviations from this climatology; The residual term "Res" contains the non-linear transient processes associated with the joint variations in water vapor content and circulation. The terms $\langle -V' \cdot \nabla \bar{q} \rangle$ and $\langle -\omega' \partial_p \bar{q} \rangle$ represent the dynamic contributions (or effect) and refer to the moisture advection induced by the horizontal wind and by the vertical pressure velocity, respectively. The terms $\langle -\bar{V} \cdot \nabla q' \rangle$ and $\langle -\bar{\omega} \partial_p q' \rangle$ represent the thermodynamic contributions (or effect), and refer to the contribution of water vapor.

https://doi.org/10.5194/egusphere-2024-1257
Preprint. Discussion started: 6 May 2024

2.2.3 Diagnosis of the MSE budget

The MSE equation is defined as follows:

$$\langle \partial_t (c_v T + L_v T) \rangle + \langle V \cdot \nabla M \rangle + \langle \omega \partial_p m \rangle = F_{net} \quad (6)$$

where the moist enthalpy is

$$M = c_p T + L_v q \quad (7)$$

and the MSE is

$$m = c_p T + L_v q + \Psi \quad (8)$$

In equations 7 and 8, c_p (c_v) represent the specific heat at constant pressure (the specific heat at constant volume); T is the air temperature and Ψ the geopotential. F_{net} is the net energy entering the atmospheric column at the surface and top of the atmosphere (latent heat, sum of sensible heat, and shortwave and longwave radiative fluxes). Similar to the moisture flux equation, the first term on the left of equation 6 can be neglected given its small variation over time on a monthly scale. The remainder of equation 6 can be decomposed into horizontal and vertical advection components, as described by:

$$\langle \omega' \partial_p \bar{m} \rangle = -\langle \bar{V} \cdot \nabla M' \rangle - \langle V' \cdot \nabla \bar{M} \rangle - \langle \omega \partial_p m' \rangle + F'_{net} + Res \quad (9)$$

Anomalous vertical motion is analyzed using this equation with a given profile of $\bar{m}$. Similar to the convention adopted for decomposing the moisture flux, the term $-\langle V' \cdot \nabla \bar{M} \rangle$ relates to the anomalous MSE associated with the atmospheric circulation and contains the dynamic contribution (or effect), while the two terms $-\langle \bar{V} \cdot \nabla M' \rangle$ and $-\langle \omega \partial_p m' \rangle$ refer to the thermodynamic contribution (or effect), which is crucial for diagnosing the thermal state of the atmosphere associated with the increase in the vertical rise of the air.

3 Diabatic heating and extreme rainfall

As mentioned earlier, the increase in SSTs in the eastern Atlantic has been identified as one of the causes of the positive precipitation anomalies in West Central Africa during October 2019 (Nicholson et al. 2022). The warming contrast between the ocean and the continent can lead to significant diabatic heating over the continent, thereby favoring atmospheric instability (Pokam et al. 2014).

Figure 1 represents the mean vertical profile (pressure-latitude) of diabatic heating averaged between 6° and 20°E during SON for the 1988-2017 climatology (Fig. 1a) and the corresponding

https://doi.org/10.5194/egusphere-2024-1257
Preprint. Discussion started: 6 May 2024

profile for 2019 (Fig. 1b). During SON, the main source of heat is located between 3°S and 9°N for climatology, and between 5°S and 13°N for 2019.

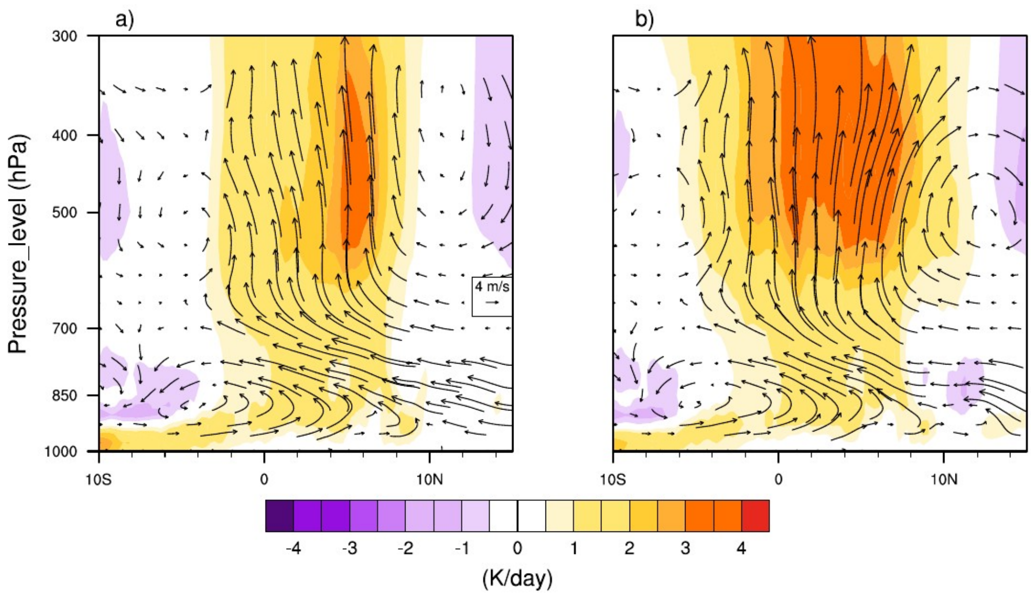

Fig 1. Diabatic heating and divergent meridional circulation (vectors; $m s^{-1}$) during the SON season for a) the 1988-2017 climatology and b) the 2019 mean, all averaged between the 6° and 20°E. As the vertical velocity is much weaker than the meridional wind, its values have been enhanced by a factor 600 for the clarity of the graph.

However, 2019 presents a more extensive and pronounced source of heat compared with the climatology 1988-2017. A 3-4 $K\,day^{-1}$ heating, more intense in 2019, occurred from 600 hPa. A cooling of 1- 2 $K\,day^{-1}$ took place around 850 hPa in the south and from 550 hPa in the north. The profound heating observed from 600 hPa originates at the surface on the southern portion of the domain (10°S). It is reinforced by the contrast between the large positive values and the negative values on either side of the equator between 500 and 400 hPa. The vertical structure of the divergent circulation is also illustrated in Figure 1. The divergent circulation appears more pronounced from 550 hPa in 2019 (Fig. 1b) compared with the climatology of 1988-2017 (Fig. 1a). This is consistent with the warming contrast observed. This uplift was reinforced by the warming of the equatorial Atlantic associated with an abnormally strong thermal low over the Sahara, which led to an acceleration of the dominant meridional flow in the divergent circulation. This is in agreement

https://doi.org/10.5194/egusphere-2024-1257
Preprint. Discussion started: 6 May 2024

with Nicholson et al. (2022), who highlighted that the West African monsoon was late to withdraw in 2019.

Although the SON season has shown significant diabatic heating compared to climatology, October 2019 in particular over West Central Africa recorded extremes of rainfall (Nicholson et al. 2022). In this study, we use the ERA5 reanalysis precipitation fields for water balance analysis. This ensures that all the examined physical quantities are consistent across the study. Before doing so, we assessed the performance of ERA5 in detecting the extreme precipitation events in October 2019. Figure 2 illustrates the interannual variability of October rainfall anomalies over West Central Africa for the period 1987-2021.

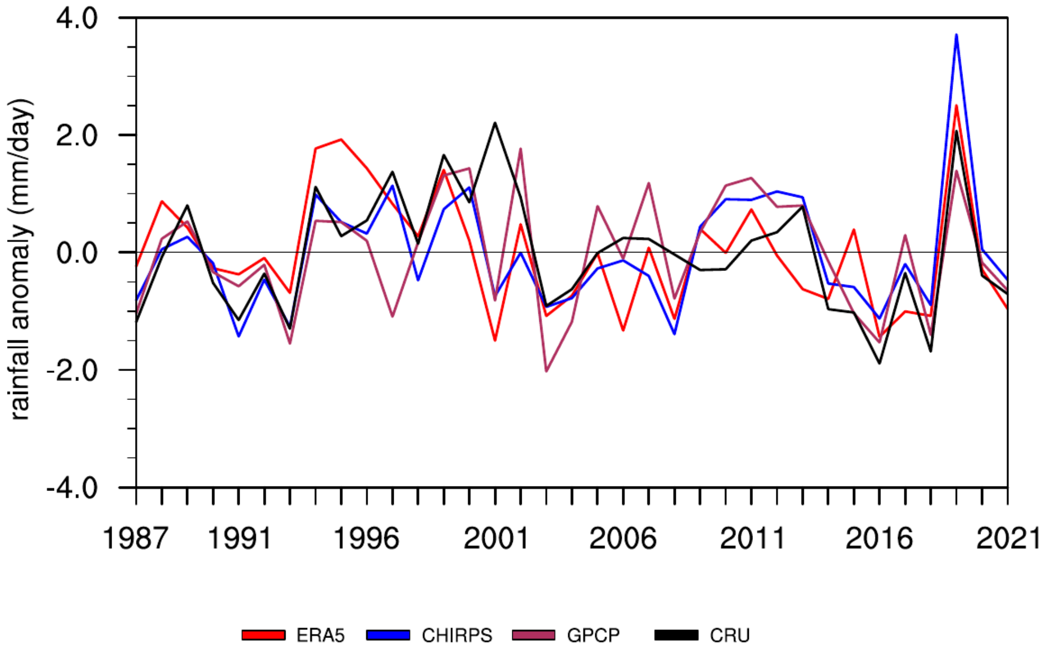

Fig 2. Temporal evolution of October rainfall anomaly over West Central Africa, from the ERA5 reanalysis dataset (red) and from observational data CHIRPS (blue), GPCP (maroon) and CRU (black), covering the period 1987–2021.

The ERA5 reanalysis (red) and the CHIRPS (blue), GPCP (maroon) and CRU (black) observations are consistent in highlighting the high precipitation peak of 2019. CHIRPS shows the highest values of positive anomalies of up to 3.5 mm day^{-1}, while ERA5 shows values of up to 2.5 mm day^{-1}.

https://doi.org/10.5194/egusphere-2024-1257
Preprint. Discussion started: 6 May 2024

Despite some differences between ERA5 and the observations in representing trends on an interannual scale (Kenfack et al. 2024), the unprecedented event of October 2019 was well detected.

The increase in SSTs in the equatorial Atlantic reached a record level during October 2019. This may have resulted in an increased specific humidity over land. Figure 3 depicts the vertical profile (pressure level-latitude) of specific humidity (colors) and meridional wind (contours) averaged between 6° and 20°E for the 1988-2017 climatology (Fig. 3a), the October 2019 average (Fig. 3b), and the October 2019 anomaly (Fig. 3c).

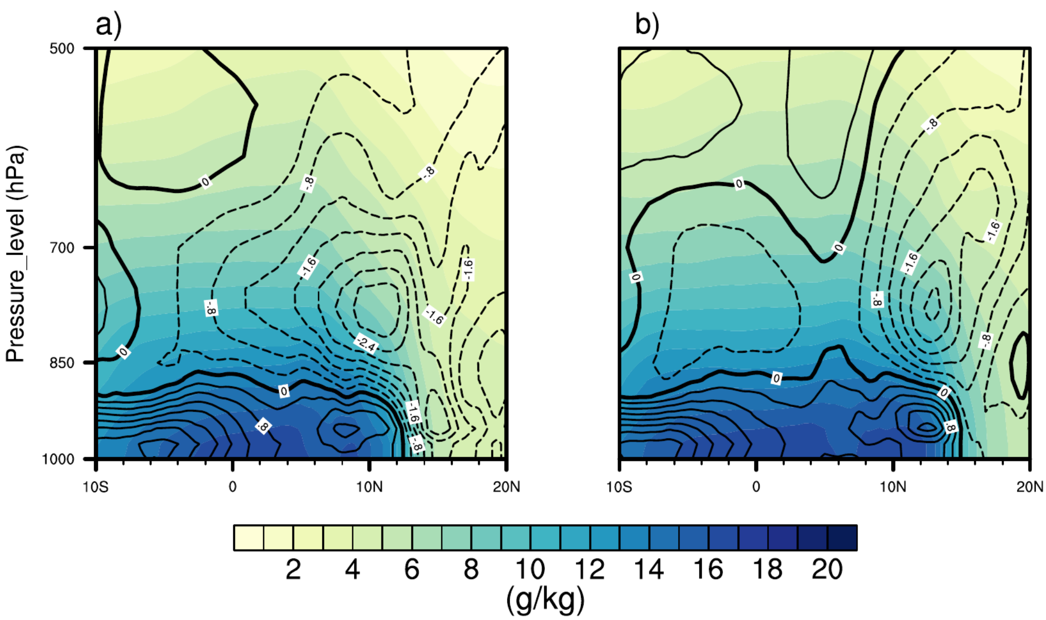

https://doi.org/10.5194/egusphere-2024-1257
Preprint. Discussion started: 6 May 2024

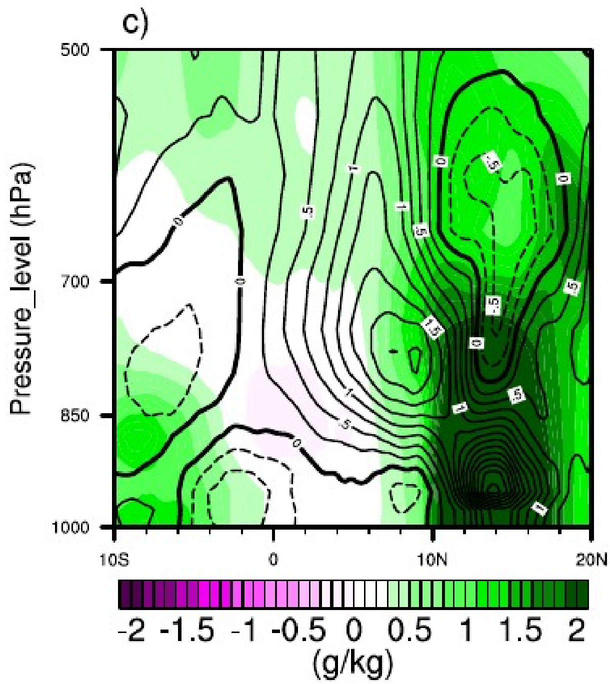

Fig. 3. Specific humidity and meridional wind (contours: m/s) in October for a) the climatology of 1988-2017, b) 2019 and c) the anomaly, averaged between 6°-20°E.

The 1988-2017 climatology is characterized by intense surface specific humidity extending as far as 12°N, whereas the October 2019 average appears to extend further to 15°N. In addition, the southerly wind in 2019 was more pronounced up to 15°N compared to the climatology. Anomaly analysis confirms that there was more moisture in equatorial central Africa in October 2019 compared to the climatology. The intensification of the southerly wind up to 15°N indicates that this moisture probably comes from the equatorial Atlantic. This is in agreement with Kamae et. al (2017), who highlighted that extreme precipitation can be a consequence of changes in humidity. Indeed, the increase in humidity associated with a substantial heating source contributes to an increase in precipitation. In addition, Chadwick et al. (2016) showed that increased humidity over land would be a response to increased moisture advection from the oceans under warming.

4 Moisture budget analysis

https://doi.org/10.5194/egusphere-2024-1257
Preprint. Discussion started: 6 May 2024

Rainfall variability in equatorial Central Africa is strongly dependent on the moisture inputs associated with atmospheric circulation (Jackson et al., 2009; Cook and Vizy, 2016, 2022; Dyer et al., 2017; Longandjo and Raoul, 2024). In the Congo Basin, heating sources combined with the vertical advection of moisture induced by anomalous vertical motion are responsible for most of the interannual variability of precipitation (Kenfack et al., 2024). In this section, we decompose the moisture budget in equation 5 to examine the processes that led to the October 2019 extreme rainfall over West Central Africa. To do this, we analyze local variations in rainfall associated with atmospheric moisture introduced into the air column by atmospheric circulation.

The monthly anomalies of the different components of the water balance averaged over West Central Africa (6°S-14°N, 6°-20°E) for October 2019 (Fig. 4) indicate that the increase in rainfall was dominated by the increase in dynamic processes.

https://doi.org/10.5194/egusphere-2024-1257
Preprint. Discussion started: 6 May 2024

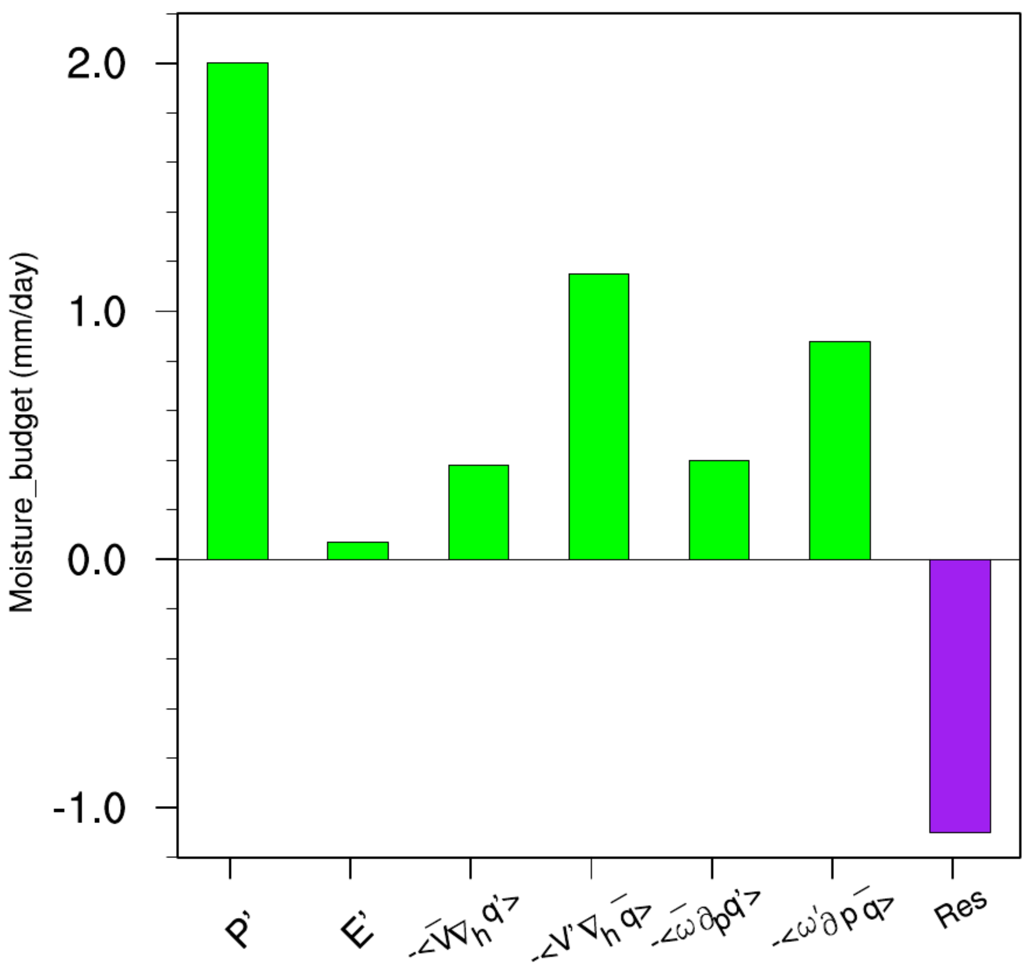

Fig. 4. Monthly mean anomalies in moisture budget for October 2019, averaged over West Equatorial Africa (6°S-14°N, 6°-20°E) as indicated by the red box in Fig. 2a.

Horizontal advection of moisture induced by the horizontal wind anomaly $\langle -V'\cdot\nabla\bar{q}\rangle$ was the most pronounced component (up to 1.2 mm/day), followed by the vertical advection of moisture induced by the vertical velocity anomaly $\langle -\omega'\partial_p\bar{q}\rangle$ (1 mm/day). Although thermodynamic processes $\langle -\bar{V}\cdot\nabla q'\rangle$ and $\langle -\bar{\omega}\partial_p q'\rangle$ are weaker than dynamic processes, they also contributed to the extreme rainfall amounts. Evaporation *E*, for its part, contributed very little (0.1 mm/day). This is consistent with Cook et al. (2019) who found that rainfall anomalies in equatorial Central

https://doi.org/10.5194/egusphere-2024-1257
Preprint. Discussion started: 6 May 2024

Africa do not depend directly on surface heating. It should also be noted that the residual term for a value of -1.1 mm/day is considerable. This could be due to the fact that the Madden-Julian Oscillation (MJO) was active over Africa, particularly in October (Wainwright et al, 2020), which probably developed nonlinear oscillatory weather systems.

At the pixel scale, positive precipitation anomalies over eastern Nigeria, southern Chad and northern Cameroon (Fig. 5a) were mainly dominated by horizontal moisture advection induced by the horizontal wind anomaly (Fig. 5d). Over Gabon, south of Congo Brazzaville, positive precipitation anomalies were dominated by vertical moisture advection induced by vertical anomalous motion (Fig. 5f). Horizontal moisture advection induced by the specific humidity anomaly (Fig. 5c), although not the key factor associated with precipitation patterns, shows a small positive contribution over the northern part of the domain.

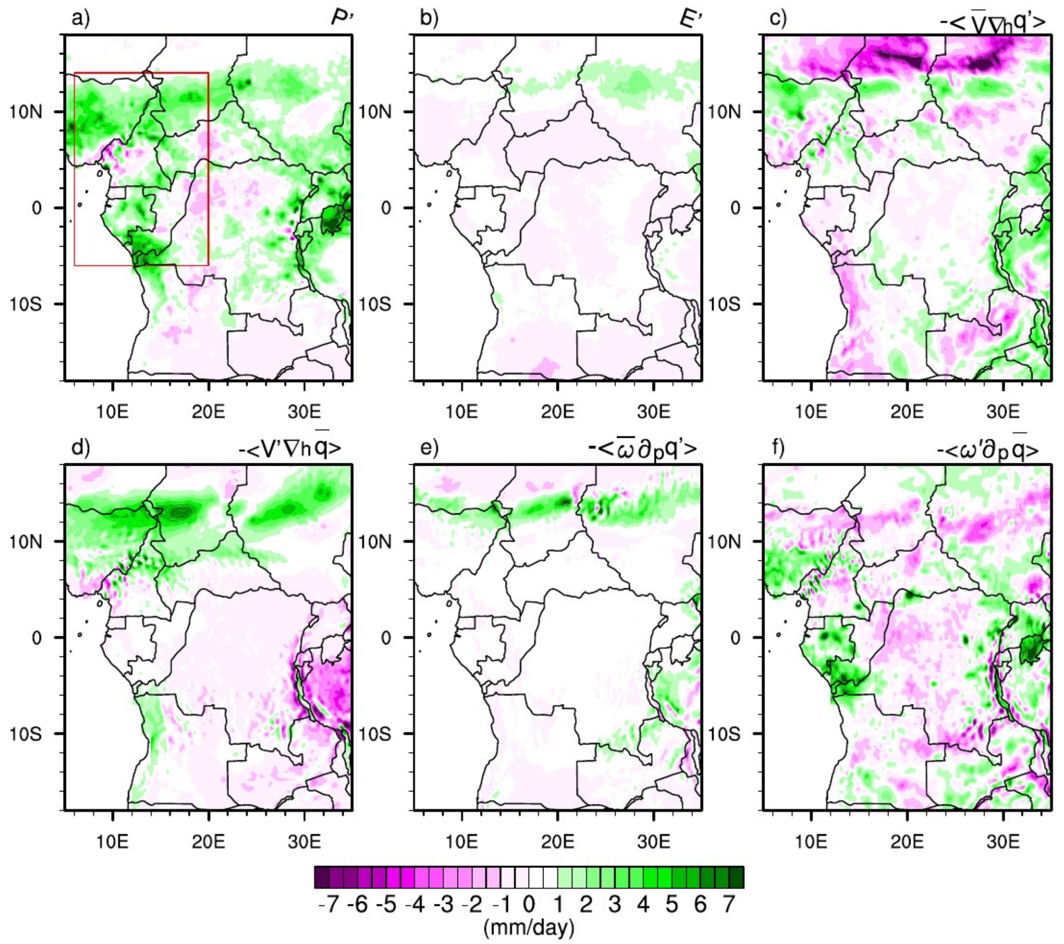

https://doi.org/10.5194/egusphere-2024-1257
Preprint. Discussion started: 6 May 2024

Fig. 5. Spatial distributions of each term of the water budget equation during October 2019 over West Equatorial Africa. (a) Precipitation anomalies, (b) evaporation anomaly, (c) horizontal advection of anomalous moisture by climatological wind, (d) horizontal advection of climatological moisture by anomalous wind, (e) vertical advection of anomalous moisture by climatological vertical velocity and (f) vertical advection of climatological moisture by anomalous vertical velocity.

The contribution of evaporation (Fig. 5b) and horizontal advection of moisture induced by the specific humidity anomaly (Fig. 5e) remains weak over the entire domain, although some positive values can be seen around 14°N. Thermodynamic effects reflect the change in the thermal state of the atmosphere associated with the October 2019 rainfall extremes over West Central Africa. It should be noted that changes in the thermal state of the atmosphere may allow us to speculate on the potential role of global warming in rainfall variations in 2019, even without considering potential impacts on atmospheric dynamics. However, changes in the thermodynamic effect, although not the key factor responsible for the October 2019 events, contributed up to 27.5% of the total effect (the sum of dynamic and thermodynamic contributions). This could be due to the increase in atmospheric humidity on the one hand and the increase in diabatic heating on the other. The increase in atmospheric humidity could be related to the increase in SSTs in the equatorial Atlantic at the same time of year as highlighted by Nicholson et al. (2022).

5 MSE budget analysis

The previous results clearly showed that the vertical advection of moisture induced by the vertical velocity anomaly was identified as the second dynamic parameter contributing to the increase in precipitation in October 2019. To better understand the creation and maintenance of the structure of vertical motion, we can base ourselves on the diagnosis of the MSE budget, which takes into account the thermal state of the atmosphere as well as the effect of atmospheric circulation. The structure of vertical motion is largely influenced by the MSE. In addition, diagnosis of the MSE balance emphasizes the relative contributions of temperature, specific humidity and atmospheric circulation associated with the vertical motion anomaly.

The vertical profiles of the vertical velocity anomaly ω' and the MSE climatology $\bar{m}$ are shown in Figure 6a.

https://doi.org/10.5194/egusphere-2024-1257
Preprint. Discussion started: 6 May 2024

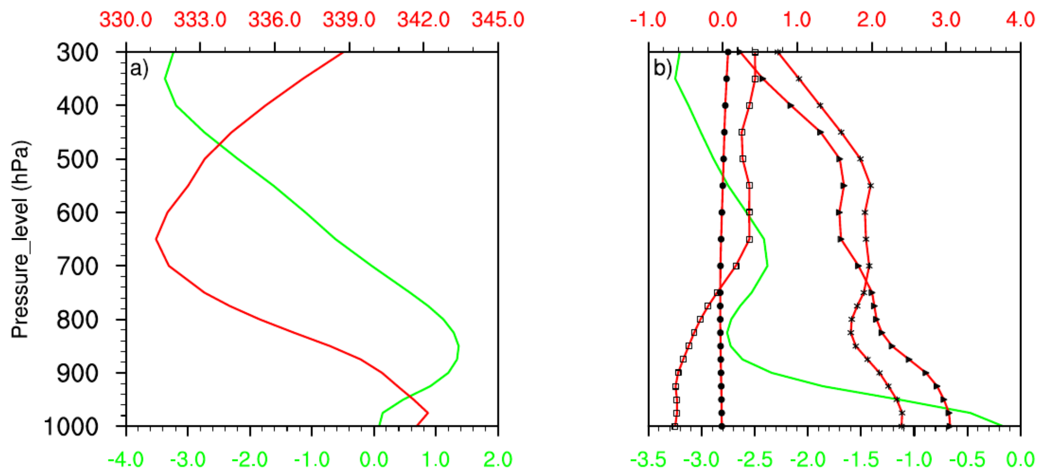

Fig. 6. Vertical profile of a) vertical velocity anomaly ω' (green line: $10^{-2} Pa.s^{-1}$) and MSE climatology $\bar{m}$ (red line: $10^{3} J.Kg^{-1}$), and b) vertical velocity climatology $\bar{\omega}$ (green line: $10^{-2} Pa.s^{-1}$), MSE anomaly m' (line with stars: $10^{3} J.Kg^{-1}$), enthalpy anomaly $c_p T'$ (line with squares: $10^{3} J.Kg^{-1}$), latent energy anomaly $l_v q'$ (line with triangles: $10^{3} J.Kg^{-1}$) and geopotential anomaly Ψ' (line with dark circle: $10^{3} J.Kg^{-1}$) averaged over West Central Africa during October 2019.

The vertical velocity anomaly ω' shows positive values at the surface and negative values in the middle and upper troposphere. The alternation of positive and negative values in the tropospheric column probably reduces the contribution of the vertical advection of moisture induced by the anomalous vertical motion. The MSE climatology $\bar{m}$ exhibits a bottom-heavy bove structure with a maximum around 650 hPa. Such a structure generally indicates that $\langle \partial_p \bar{m} \rangle < 0$ (Chen and Bordoni, 2014; Liu et al. 2021; Wen et al. 2022). As a result, positive (negative) values of $\langle \omega' \partial_p \bar{m} \rangle$ indicate anomalous ascending (descending) motion over West Central Africa. The vertical velocity climatology $\bar{\omega}$ (Fig. 6b) is negative over the entire troposphere, characterizing an upward movement. The MSE anomaly m' decreased near the surface then increased from 800 hPa to 550 hPa, with a maximum value around 650 hPa. However, this includes three terms, namely, gz'

https://doi.org/10.5194/egusphere-2024-1257
Preprint. Discussion started: 6 May 2024

which is weak in the entire tropospheric column, the enthalpy anomaly $c_p T'$, which tends to increase, and $l_v q'$, which approaches m'.

Based on the contributions of the different terms in equation 9 to the MSE averaged over West Central Africa (Fig. 7), the advection of wet enthalpy induced by the horizontal wind anomalies $-\langle V' \cdot \nabla \bar{M} \rangle$ is the main term contributing most to the vertical advection of the MSE induced by the vertical velocity anomaly $\langle \omega' \partial_p \bar{m} \rangle$.

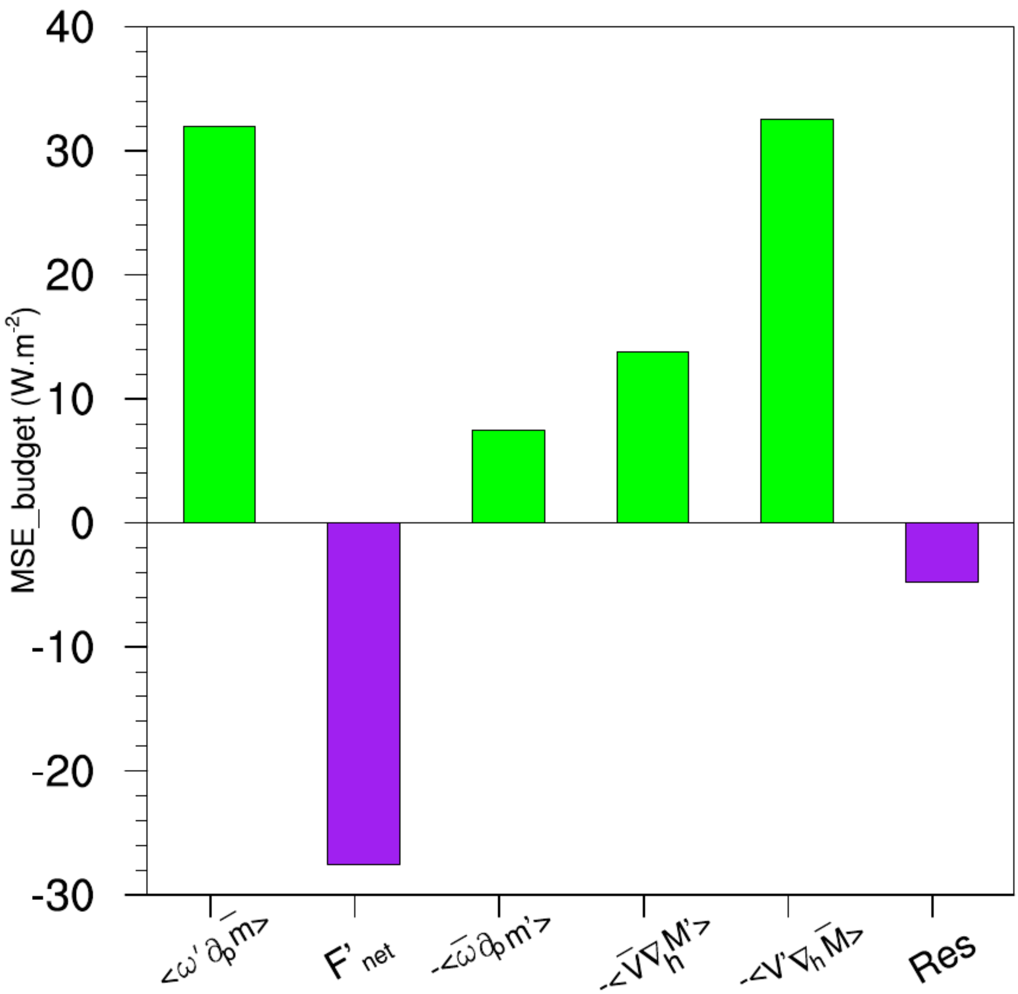

Fig. 7. Different terms of the Moist Static Energy (MSE) budget averaged over West Equatorial Africa.

https://doi.org/10.5194/egusphere-2024-1257
Preprint. Discussion started: 6 May 2024

We also note the contribution of the thermodynamic terms, although the horizontal advection of the MSE induced by the wet enthalpy variation $-\langle \bar{V} \cdot \nabla M' \rangle$ dominates compared to the vertical advection of the MSE induced by the MSE variation $-\langle \omega \partial_p m' \rangle$. A reduction in the net energy flux is noticeable. This could be due to the fact that the energy in the radiative and turbulent heat fluxes penetrating the atmosphere over West central Africa has suffered a loss linked to the increase in cloud cover, which has a strong influence on short-wave radiation. Such a reduction in energy in the air column has an impact on upward motion. This result is in line with that of Wen et al. (2022) and Sheng et al. (2023) , who pointed to a reduction in the net energy in the air column during the exceptional rainy season in the summer of 2020 in the Yangtze river valley and the anomalous increase in precipitation over southern China in 2022. However, the residual term is weak.

On a regional scale, the vertical advection of the MSE induced by the vertical motion anomaly $\langle \omega' \partial_p \bar{m} \rangle$ (Fig. 8a) is mainly dominated by the dynamic term $-\langle V' \cdot \nabla \bar{M} \rangle$ (Fig. 8c), which brings moist enthalpy into the domain.

https://doi.org/10.5194/egusphere-2024-1257
Preprint. Discussion started: 6 May 2024

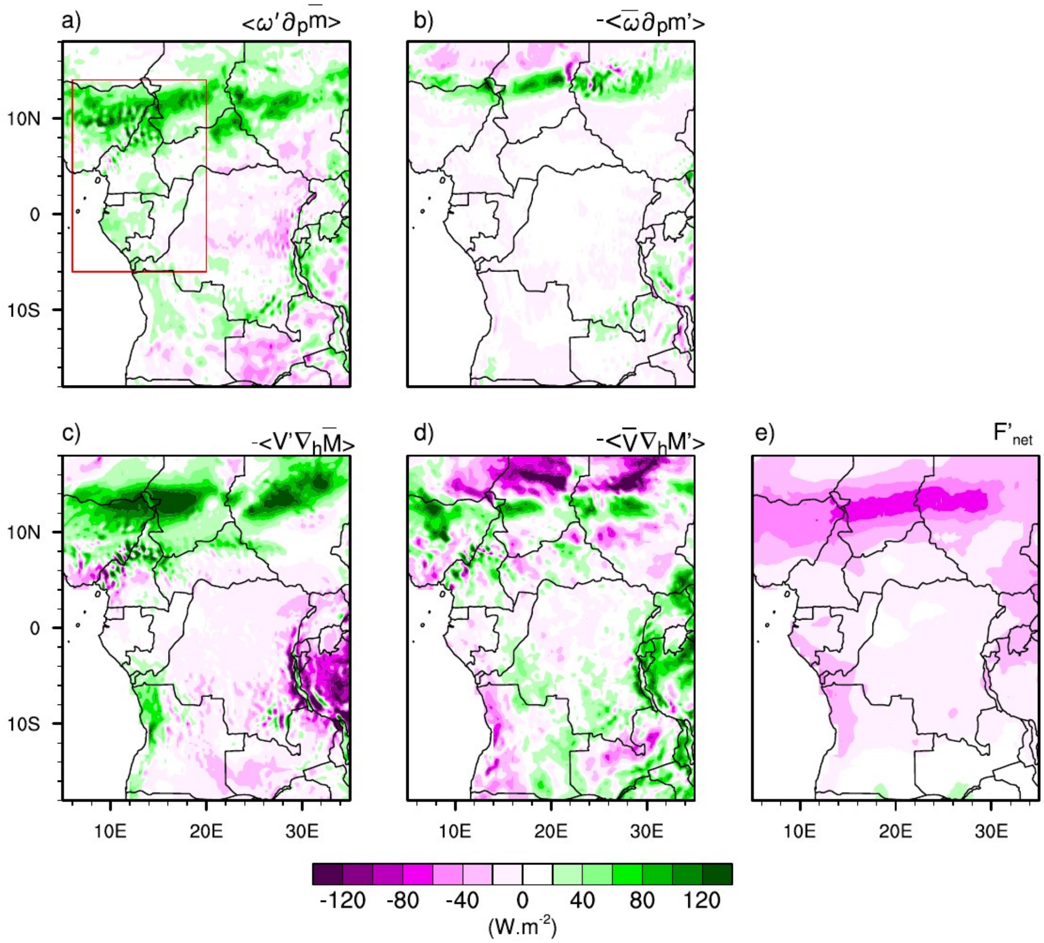

Fig. 8. Spatial distributions of each term of the Moist Static Energy (MSE) balance equation during October 2019 over West Equatorial Africa. (a) vertical advection of climatological MSE by anomalous vertical velocity, (b) vertical advection of anomalous MSE by climatological vertical velocity, (c) horizontal advection of anomalous moist enthalpy by climatological wind, (e) horizontal advection of climatological moist enthalpy by anomalous wind, and (f) net energy flux (at the surface and top of the atmosphere) in the atmospheric column.

There is a high concentration of positive values in both dynamic terms, up to 120 $W \cdot m^{-2}$ in the north of West Central Africa. In addition, the two thermodynamic terms $-\langle \bar{\omega} \partial_p m' \rangle$ (Fig. 8b) and $-\langle \bar{V} \cdot \nabla M' \rangle$ (Fig. 8d), although weak, also contributed to reinforcing the vertical advection of

https://doi.org/10.5194/egusphere-2024-1257
Preprint. Discussion started: 6 May 2024

MSE induced by the vertical motion anomaly. It should be remembered that the term $-\langle \omega \partial_p m' \rangle$ remains very weak over the region as a whole, with the exception of the northern part where a slight layer of positive values can be observed. Terms $-\langle V' \cdot \nabla \bar{M} \rangle$, $-\langle \bar{V} \cdot \nabla M' \rangle$ and $-\langle \omega \partial_p m' \rangle$ in the MSE have a similar spatial distribution to terms $\langle -V' \cdot \nabla \bar{q} \rangle$, $\langle -\bar{V} \cdot \nabla q' \rangle$ and $\langle -\bar{\omega} \partial_p q' \rangle$ in the moisture, which is in agreement with the findings of Kenfack et al. (2024). The difference between the net energy balance for 2019 and the climatology (Fig. 8e) shows negative values for the whole of the region. The MSE balance indicates a pronounced net energy reduction in the atmospheric column over the Sahel, which results in a decrease in the vertical advection of moisture induced by the anomalous vertical motion. Although the dynamic contribution is the most important, the thermodynamic contribution cannot be neglected. This would mean that feedbacks between atmospheric dynamic and thermodynamic variables would induce significant indirect effects on October 2019 precipitation anomalies over West Central Africa.

5.1 Dynamic effect

The aforementioned results clearly show that enthalpy advection induced by the horizontal wind anomaly is crucial in understanding the processes at the origin of October 2019 extreme precipitation over West Central Africa. It should be remembered that, as we mentioned in the diagnostic section of the MSE balance, the wet enthalpy $M = c_p T + L_v q$ results from the sum of the dry enthalpy and the latent heat. Thus, the horizontal advection of wet enthalpy induced by the wind anomaly can be separated into two terms: dry enthalpy $-\langle V' \cdot \nabla_h c_p T \rangle$ (Fig. 9a) and latent heat $-\langle V' \cdot \nabla_h l_v \bar{q} \rangle$ (Fig. 9d).

https://doi.org/10.5194/egusphere-2024-1257
Preprint. Discussion started: 6 May 2024

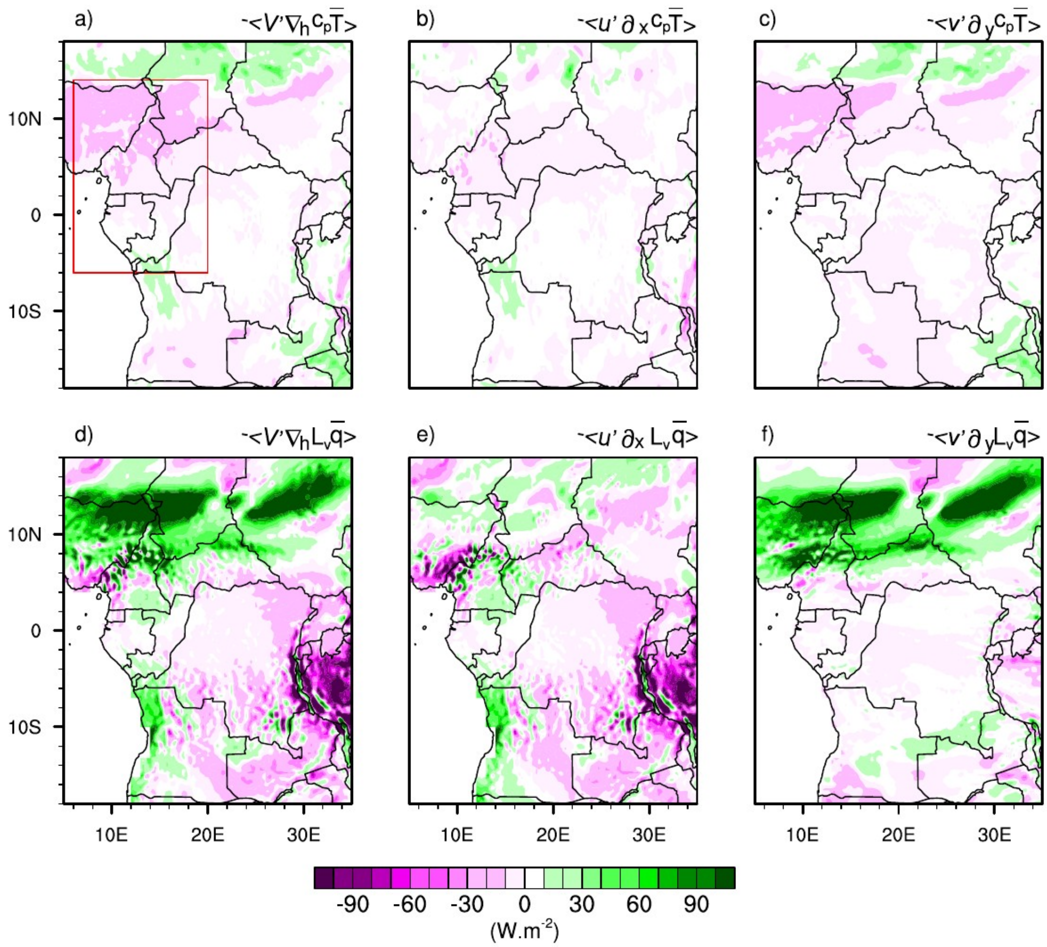

Fig. 9. Horizontal advection of (a–c) climatological dry enthalpy and (d–f) latent energy by anomalous wind, designated as a dynamic effect during October 2019 over West Central Africa. (a, d) Total advection, (b, e) zonal component, and (c, f) meridional component.

Given the influence of the wind anomaly components on the displacement of dry enthalpy and latent heat, a further decomposition of the $-\langle V' \cdot \nabla_h c_p \bar{T} \rangle$ and $-\langle V' \cdot \nabla_h l_v \bar{q} \rangle$ terms along the zonal (Figs. 9b,e) and meridional (Figs. 9c,f) directions appears necessary. Figure 9a shows that the advection of dry enthalpy induced by the horizontal wind anomaly decreased over the entire domain, with the highest values between 6°N and 14°N. The advection of dry enthalpy by the meridional wind anomaly (Fig. 9c) is particularly responsible for the decrease in the

https://doi.org/10.5194/egusphere-2024-1257
Preprint. Discussion started: 6 May 2024

$-\langle V'\cdot\nabla_h c_p T\rangle$ term compared with the advection of dry enthalpy induced by the zonal wind anomaly (Fig. 9b), which is weak. For the transport of latent heat (Fig. 9d), the influence of the advection of $-\langle V'\cdot\nabla_h l_V \bar{q}\rangle$ term under the effect of the anomalous meridional circulation is the main term responsible for the supply of moist air to the northern part of the area, while the low contribution to the south is associated with a low input of moist air from the zonal wind anomaly (Fig. 9f). Analysis of the advection of dry enthalpy and latent heat by anomalous winds shows that the meridional wind anomaly had a significant impact compared with the zonal wind anomaly. In addition, the advection of the dynamic term associated with latent heat contributed significantly to the supply of moist air to West Central Africa compared to the advection of the dynamic term associated with dry enthalpy.

5.2 Thermodynamic effect

The results of the previous section highlighted the importance of dynamics, particularly in a meridional direction, on extreme precipitation in October 2019. However, we previously also observed that the thermodynamic contribution should not be neglected (Fig. 8d). Similar to the previous section, the thermodynamic term $-\langle \bar{V}\cdot\nabla M'\rangle$ (i.e. the advection of the wet enthalpy anomaly associated with wind climatology) can also be separated into two terms, namely: Dry enthalpy $-\langle \bar{V}\cdot\nabla_h c_p T'\rangle$ (Fig. 10a) and latent heat $-\langle \bar{V}\cdot\nabla_h l_V \bar{q}'\rangle$ (Fig. 10d).

https://doi.org/10.5194/egusphere-2024-1257
Preprint. Discussion started: 6 May 2024

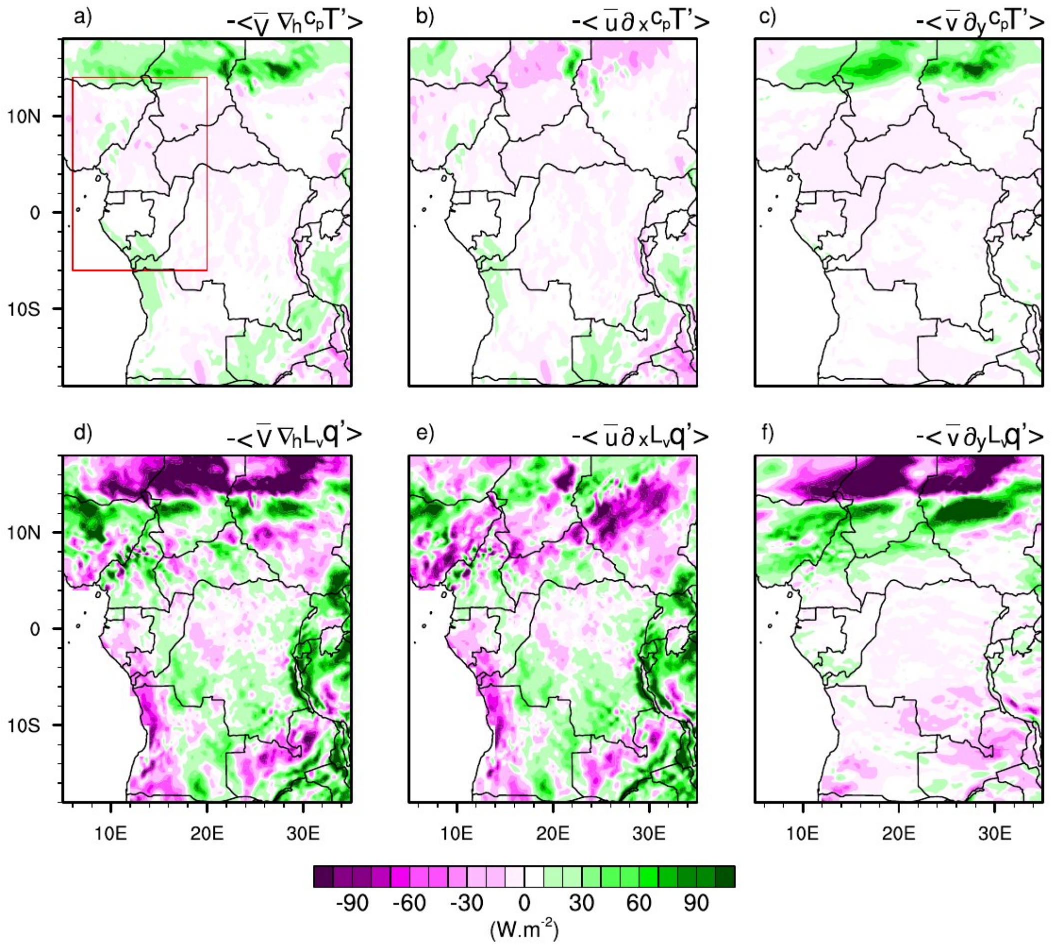

Fig. 10. As in Fig. 9, but for the thermodynamic effect (horizontal advection of anomalous dry enthalpy and latent energy by climatological wind) during October 2019 over West Central Africa.

To better assess the contribution of each term, we split the horizontal wind into zonal and meridional directions. The advection of the dry enthalpy anomaly by the horizontal zonal and meridional wind components is shown in Figures 10 b and 10c, respectively. It can also be seen that the dry enthalpy anomaly is very small over the whole area. On the other hand, the advection of the latent heat anomaly by the horizontal wind climatology is more pronounced. Variations in latent heat are strong in the meridional direction, while the zonal direction shows a reduction in abnormal latent heat. This could be due to the warming of the equatorial Atlantic, which results in strong advection of water vapor into West Central Africa, leading to precipitation. The reduction in

https://doi.org/10.5194/egusphere-2024-1257
Preprint. Discussion started: 6 May 2024

advection of the latent heat anomaly on the Atlantic coast is amplified by the zonal wind climatology. However, the advection of the wet enthalpy induced by the horizontal wind anomaly (dynamic effect) is stronger than the advection of the wet enthalpy anomaly by the wind climatology. As a result, we note in particular the changes in the meridional wind for the dynamic effect and the latent heat associated with the warming of the equatorial Atlantic for the thermodynamic effect.

6 Summary and concluding remarks

West Central Africa was hit by unprecedented exceptional rainfall in October 2019. A few studies have investigated the meteorological causes associated with these extreme rainfall events (Wainwright et al, 2020; Nicholson et al. 2022). This study followed these perspectives and focused on evaluating the dynamic and thermodynamic processes that controlled the extreme events of 2019. We proceeded by decomposing the water balance and MSE equation, separating the associated dynamic and thermodynamic effects. Changes in atmospheric circulation are behind dynamic processes, while changes in water vapor are behind thermodynamic processes. This approach provides a better understanding of the mechanisms behind rainfall anomalies. The thermodynamic effect, in particular, can be exploited to estimate the impact of global warming on the heavy precipitation of October 2019, notably on the increase in the temperature of the troposphere and its water vapor content. The main findings can be summarized as follows:

1. The main feature of October 2019 was a strong southerly circulation compared with the typical climatology for 1988-2017. In addition, a more pronounced rate of humidity associated with significant diabatic heating over West Central Africa up to 15°N were recorded.
2. The diagnosis of the water balance reveals that the exceptional rainfall in October 2019 is mainly dominated by dynamic effects. However, moisture advection induced by horizontal wind anomalies controls precipitation anomalies in the north of the area, while vertical moisture advection induced by vertical velocity anomalies controls precipitation extremes in the south, mainly over Gabon and southern Congo Brazzaville. Changes in the thermodynamic effect, although not the key factor responsible for the events of October 2019, contribute up to 27.5% of the total effect (the sum of the dynamic and thermodynamic contributions). The contribution of evaporation remains weak, which allows us to conclude that evaporation was not responsible for the heavy rainfall of October 2019 in West Central Africa.

https://doi.org/10.5194/egusphere-2024-1257
Preprint. Discussion started: 6 May 2024

3. The vertical advection of the MSE was controlled by the dynamic term (i.e. the advection of the wet enthalpy induced by the horizontal wind anomalies) compared to the thermodynamic terms (i.e. the horizontal advection of the MSE induced by the variation of the wet enthalpy and the vertical advection of the MSE induced by the variation of the MSE). These variations in the MSE were governed by its meridional component, in particular the variations in the meridional wind in the dynamic effect and the meridional variations in latent heat in the thermodynamic effect. It should be pointed out that in both cases, the contribution of dry enthalpy helped to reduce the dynamic term and was small in the thermodynamic term.

The results of this study show that moisture advection induced by horizontal wind anomalies and vertical moisture advection induced by vertical velocity anomaly were crucial mechanisms on the anomalous October 2019 exceptional rainfall increase over West Central Africa. In addition, changes in the MSE budget, mainly through the meridional circulation (dynamic effect), and latent heat (thermodynamic effect) also played an important role. However, there was little contribution from dry enthalpy. These results are consistent with those of Nicholson et al (2021) who showed that the increase in equatorial Atlantic SSTs associated with the late retreat of the West African monsoon played an important role in precipitation anomalies in the Sahel. The importance of the dynamic contribution during extreme precipitation events has been reported in other regions, notably over southern China (Wen et al. 2022; Sheng et al. 2023). This calls for comprehensive evaluations of both dynamic and thermodynamic contributions, and their possible feedback, to assess the potential impact of climate change on extreme precipitation events in this region.

Acknowledgements. The authors thank all the observational and reanalysis data providers used in this study, and the research of the International Joint Laboratory “Dynamics of Terrestrial Ecosystems in Central Africa: A Context of Global Changes” (IJL DYCOCA/LMI DYCOFAC).

Competing Interests. The authors declare that they have no conflict of interest.

Authors' contributions

kevin Kenfack: Conceptualization; data analysis; formal analysis; investigation; methodology; writing - original draft; review and editing.

Francesco Marra: Supervision; conceptualization; investigation; writing – review and editing.
Zéphirin Yepdo Djomou: Investigation; writing; review and editing; supervision; validation.
Lucie A. Djiotang Tchotchou: Validation; supervision; methodology; writing – review and editing.
Alain T. Tamoffo: Conceptualization; investigation; methodology; project administration; resources; supervision; validation; review and editing.
Derbetini A. Vondou: Project administration; supervision; resources; validation; methodology; writing – review and editing.

Funding. Not applicable

Data Availability Statement

The **ERA5** reanalysis is produced within the Copernicus Climate Change Service (C3S) by the ECMWF and is accessible via the link https://cds.climate.copernicus.eu/cdsapp#!/dataset/reanalysis-era5-pressure-levels-monthly-means?tab1⁄4form.

References

Andrews, P. C., Cook, K. H., & Vizy, E. K. (2023). Mesoscale convective systems in the Congo Basin: Seasonality, regionality, and diurnal cycles. *Climate Dynamics*, *62*(1), 609–630. https://doi.org/10.1007/s00382-023-06903-7

Aretouyap, Z., Kemgang, F. E. G., Domra, J. K., Bisso, D., & Njandjock, P. N. (2021). Understanding the occurrences of fault and landslide in the region of West-Cameroon using remote sensing and GIS techniques. *Natural Hazards*, *109*(2), 1589–1602. https://doi.org/10.1007/s11069-021-04890-8

Bell, J. P., Tompkins, A. M., Bouka-Biona, C., & Sanda, I. S. (2015). A process-based investigation into the impact of the Congo basin deforestation on surface climate. *Journal of Geophysical Research: Atmospheres*, *120*(12), 5721–5739. https://doi.org/10.1002/2014jd022586

Black, E. (2005). The relationship between Indian Ocean sea–surface temperature and East African rainfall. *Philosophical Transactions of the Royal Society A: Mathematical, Physical and Engineering Sciences*, *363*(1826), 43–47. https://doi.org/10.1098/rsta.2004.1474

Chadwick, R., Good, P., & Willett, K. (2016). A simple moisture advection model of specific humidity change over land in response to SST warming. *Journal of Climate*, *29*(21), 7613–7632. https://doi.org/10.1175/jcli-d-16-0241.1

Chen, J., & Bordoni, S. (2014). Orographic effects of the Tibetan plateau on the east Asian summer monsoon: An energetic perspective. *Journal of Climate*, *27*(8), 3052–3072. https://doi.org/10.1175/jcli-d-13-00479.1

Cook, K. H., Liu, Y., & Vizy, E. K. (2019). Congo Basin drying associated with poleward shifts of the African thermal lows. *Climate Dynamics*, *54*(1–2), 863–883. https://doi.org/10.1007/s00382-019-05033-3

Cook, K. H., & Vizy, E. K. (2021). Hydrodynamics of regional and seasonal variations in Congo Basin precipitation. *Climate Dynamics*, *59*(5–6), 1775–1797. https://doi.org/10.1007/s00382-021-06066-3

Dyer, E. L. E., Jones, D. B. A., Nusbaumer, J., Li, H., Collins, O., Vettoretti, G., & Noone, D. (2017). Congo Basin precipitation: Assessing seasonality, regional interactions, and sources

https://doi.org/10.5194/egusphere-2024-1257
Preprint. Discussion started: 6 May 2024

of moisture. *Journal of Geophysical Research: Atmospheres*, *122*(13), 6882–6898. https://doi.org/10.1002/2016jd026240

Fontaine, B., Roucou, P., & Trzaska, S. (2003). Atmospheric water cycle and moisture fluxes in the West African monsoon: Mean annual cycles and relationship using NCEP/NCAR reanalysis. *Geophysical Research Letters*, *30*(3). https://doi.org/10.1029/2002gl015834

Fotso-Nguemo, T. C., Chamani, R., Yepdo, Z. D., Sonkoué, D., Matsaguim, C. N., Vondou, D. A., & Tanessong, R. S. (2018). Projected trends of extreme rainfall events from CMIP5 models over Central Africa. *Atmospheric Science Letters*, *19*(2). https://doi.org/10.1002/asl.803

Fotso-Nguemo, T. C., Diallo, I., Diakhaté, M., Vondou, D. A., Mbaye, M. L., Haensler, A., Gaye, A. T., & Tchawoua, C. (2019). Projected changes in the seasonal cycle of extreme rainfall events from CORDEX simulations over Central Africa. *Climatic Change*, *155*(3), 339–357. https://doi.org/10.1007/s10584-019-02492-9

Funk, C., Peterson, P., Landsfeld, M., Pedreros, D., Verdin, J., Shukla, S., Husak, G., Rowland, J., Harrison, L., Hoell, A., & Michaelsen, J. (2015). The climate hazards infrared precipitation with stations—a new environmental record for monitoring extremes. *Scientific Data*, *2*(1). https://doi.org/10.1038/sdata.2015.66

Garcin, Y., Deschamps, P., Ménot, G., de Saulieu, G., Schefuß, E., Sebag, D., Dupont, L. M., Oslisly, R., Brademann, B., Mbusnum, K. G., Onana, J.-M., Ako, A. A., Epp, L. S., Tjallingii, R., Strecker, M. R., Brauer, A., & Sachse, D. (2018). Early anthropogenic impact on Western Central African rainforests 2,600 y ago. *Proceedings of the National Academy of Sciences*, *115*(13), 3261–3266. https://doi.org/10.1073/pnas.1715336115

Gou, Y., Balling, J., De Sy, V., Herold, M., De Keersmaecker, W., Slagter, B., Mullissa, A., Shang, X., & Reiche, J. (2022). Intra-annual relationship between precipitation and forest disturbance in the African rainforest. *Environmental Research Letters*, *17*(4), 044044. https://doi.org/10.1088/1748-9326/ac5ca0

Harris, I., Osborn, T. J., Jones, P., & Lister, D. (2020). Version 4 of the CRU TS monthly high-resolution gridded multivariate climate dataset. *Scientific Data*, *7*(1). https://doi.org/10.1038/s41597-020-0453-3

He, Y., Tian, W., Huang, J., Wang, G., Ren, Y., Yan, H., Yu, H., Guan, X., & Hu, H. (2021). The mechanism of increasing summer water vapor over the Tibetan plateau. *Journal of Geophysical Research: Atmospheres*, *126*(10). https://doi.org/10.1029/2020jd034166

Hersbach, H., Bell, B., Berrisford, P., Hirahara, S., Horányi, A., Muñoz-Sabater, J., Nicolas, J., Peubey, C., Radu, R., Schepers, D., Simmons, A., Soci, C., Abdalla, S., Abellan, X., Balsamo, G., Bechtold, P., Biavati, G., Bidlot, J., Bonavita, M., … Thépaut, J. (2020). The ERA5 global reanalysis. *Quarterly Journal of the Royal Meteorological Society*, *146*(730), 1999–2049. https://doi.org/10.1002/qj.3803

Hua, W., Zhou, L., Nicholson, S. E., Chen, H., & Qin, M. (2019). Assessing reanalysis data for understanding rainfall climatology and variability over Central Equatorial Africa. *Climate Dynamics*, *53*(1–2), 651–669. https://doi.org/10.1007/s00382-018-04604-0

Huffman, G. J., Adler, R. F., Bolvin, D. T., & Gu, G. (2009). Improving the global

https://doi.org/10.5194/egusphere-2024-1257
Preprint. Discussion started: 6 May 2024

precipitation record: GPCP Version 2.1. *Geophysical Research Letters*, *36*(17). https://doi.org/10.1029/2009gl040000

Jackson, B., Nicholson, S. E., & Klotter, D. (2009). Mesoscale convective systems over Western Equatorial Africa and their relationship to large-scale circulation. *Monthly Weather Review*, *137*(4), 1272–1294. https://doi.org/10.1175/2008mwr2525.1

Jiang, J., Zhou, T., Chen, X., & Zhang, L. (2020). Future changes in precipitation over Central Asia based on CMIP6 projections. *Environmental Research Letters*, *15*(5), 054009. https://doi.org/10.1088/1748-9326/ab7d03

Johannsen, Ermida, Martins, Trigo, Nogueira, & Dutra. (2019). Cold bias of ERA5 summertime daily maximum land surface temperature over Iberian Peninsula. *Remote Sensing*, *11*(21), 2570. https://doi.org/10.3390/rs11212570

Kamae, Y., Mei, W., & Xie, S.-P. (2017). Climatological relationship between warm season atmospheric rivers and heavy rainfall over East Asia. *Journal of the Meteorological Society of Japan. Ser. II*, *95*(6), 411–431. https://doi.org/10.2151/jmsj.2017-027

Kenfack, K., Tamoffo, A. T., Djiotang Tchotchou, L. A., & Vondou, D. A. (2023). Assessment of uncertainties in reanalysis datasets in reproducing thermodynamic mechanisms in the moisture budget’s provision in the Congo Basin. *Theoretical and Applied Climatology*, *154*(1–2), 613–626. https://doi.org/10.1007/s00704-023-04576-0

Kenfack, K., Tamoffo, A. T., Tchotchou, L. A. D., Marra, F., Kaissassou, S., Nana, H. N., & Vondou, D. A. (2024). Processes behind the decrease in Congo Basin precipitation during the

https://doi.org/10.5194/egusphere-2024-1257
Preprint. Discussion started: 6 May 2024

rainy seasons inferred from ERA-5 reanalysis. *International Journal of Climatology*. https://doi.org/10.1002/joc.8410

Kenya – over 100 dead, 18,000 displaced after recent floods and landslides – floodlist. (n.d.). Retrieved April 2, 2024, from http://floodlist.com/africa/kenya-floods-november-2019

Kuete, G., Pokam Mba, W., & Washington, R. (2019). African Easterly Jet South: Control, maintenance mechanisms and link with Southern subtropical waves. *Climate Dynamics*, *54*(3–4), 1539–1552. https://doi.org/10.1007/s00382-019-05072-w

Li, P., Zhou, T., & Chen, X. (2017). Water vapor transport for spring persistent rains over southeastern China based on five reanalysis datasets. *Climate Dynamics*, *51*(11–12), 4243–4257. https://doi.org/10.1007/s00382-017-3680-3

Liu, S., Wen, N., & Li, L. (2021). Dynamic and thermodynamic contributions to Northern China dryness in El Niño developing summer. *International Journal of Climatology*, *41*(4), 2878–2890. https://doi.org/10.1002/joc.6995

Longandjo, G.-N. T., & Rouault, M. (2024). Revisiting the seasonal cycle of rainfall over Central Africa. *Journal of Climate*, *37*(3), 1015–1032. https://doi.org/10.1175/jcli-d-23-0281.1

Mariotti, L., Diallo, I., Coppola, E., & Giorgi, F. (2014). Seasonal and intraseasonal changes of African monsoon climates in 21st century CORDEX projections. *Climatic Change*, *125*(1), 53–65. https://doi.org/10.1007/s10584-014-1097-0

https://doi.org/10.5194/egusphere-2024-1257
Preprint. Discussion started: 6 May 2024

Marra, F., Levizzani, V., & Cattani, E. (2022). Changes in extreme daily precipitation over Africa: Insights from a non-asymptotic statistical approach. *Journal of Hydrology X*, *16*, 100130. https://doi.org/10.1016/j.hydroa.2022.100130

Moon, S., & Ha, K.-J. (2020). Future changes in monsoon duration and precipitation using CMIP6. *Npj Climate and Atmospheric Science*, *3*(1). https://doi.org/10.1038/s41612-020-00151-w

Moudi Pascal, I., Kammalac Jores, T., Talib, J., Appolinaire, V. D., Hirons, L., Christian, N., Tene Romeo-Ledoux, D., Fogang Michael, T., Marceline, M., Tanessong Roméo, S., Dione, C., Thompson, E., Salih, A. A. M., & Ngaryamgaye, S. (2023). Strengthening weather forecast and dissemination capabilities in Central Africa: Case assessment of intense flooding in January 2020. *Climate Services*, *32*, 100411. https://doi.org/10.1016/j.cliser.2023.100411

Nana, H. N., Tanessong, R. S., Tchotchou, L. A. D., Tamoffo, A. T., Moihamette, F., & Vondou, D. A. (2023). Influence of strong South Atlantic Ocean Dipole on the Central African rainfall's system. *Climate Dynamics*, *62*(1), 1–16. https://doi.org/10.1007/s00382-023-06892-7

Neelin, J. D. (2021). Moist dynamics of tropical convection zones in monsoons, teleconnections, and global warming. In *The Global Circulation of the Atmosphere* (pp. 267–301). Princeton University Press. http://dx.doi.org/10.2307/j.ctv1t1kg52.14

Ngandam Mfondoum, A. H., Wokwenmendam Nguet, P., Mefire Mfondoum, J. V., Tchindjang, M., Hakdaoui, S., Cooper, R., Gbetkom, P. G., Penaye, J., Bekoa, A., & Moudioh, C. (2021). Adapting sudden landslide identification product (SLIP) and detecting

https://doi.org/10.5194/egusphere-2024-1257
Preprint. Discussion started: 6 May 2024

real-time increased precipitation (DRIP) algorithms to map rainfall-triggered landslides in Western Cameroon highlands (Central-Africa). *Geoenvironmental Disasters*, *8*(1). https://doi.org/10.1186/s40677-021-00189-9

Nicholson, S. E., Fink, A. H., Funk, C., Klotter, D. A., & Satheesh, A. R. (2022). Meteorological causes of the catastrophic rains of October/November 2019 in equatorial Africa. *Global and Planetary Change*, *208*, 103687. https://doi.org/10.1016/j.gloplacha.2021.103687

Oueslati, B., Yiou, P., & Jézéquel, A. (2019). Revisiting the dynamic and thermodynamic processes driving the record-breaking January 2014 precipitation in the southern UK. *Scientific Reports*, *9*(1). https://doi.org/10.1038/s41598-019-39306-y

Pokam, W. M., Bain, C. L., Chadwick, R. S., Graham, R., Sonwa, D. J., & Kamga, F. M. (2014). Identification of processes driving low-level westerlies in West Equatorial Africa. *Journal of Climate*, *27*(11), 4245–4262. https://doi.org/10.1175/jcli-d-13-00490.1

Pokam, W. M., Djiotang, L. A. T., & Mkankam, F. K. (2011). Atmospheric water vapor transport and recycling in Equatorial Central Africa through NCEP/NCAR reanalysis data. *Climate Dynamics*, *38*(9–10), 1715–1729. https://doi.org/10.1007/s00382-011-1242-7

Seager, R., Naik, N., & Vecchi, G. A. (2010). Thermodynamic and dynamic mechanisms for large-scale changes in the hydrological cycle in response to global warming*. *Journal of Climate*, *23*(17), 4651–4668. https://doi.org/10.1175/2010jcli3655.1

Sheng, B., Wang, H., Li, H., Wu, K., & Li, Q. (2023). Thermodynamic and dynamic effects of anomalous dragon boat water over South China in 2022. *Weather and Climate Extremes*, *40*, 100560. https://doi.org/10.1016/j.wace.2023.100560

Sonkoué, D., Monkam, D., Fotso-Nguemo, T. C., Yepdo, Z. D., & Vondou, D. A. (2018). Evaluation and projected changes in daily rainfall characteristics over Central Africa based on a multi-model ensemble mean of CMIP5 simulations. *Theoretical and Applied Climatology*, *137*(3–4), 2167–2186. https://doi.org/10.1007/s00704-018-2729-5

Taguela, T. N., Pokam, W. M., & Washington, R. (2022). Rainfall in uncoupled and coupled versions of the Met Office Unified Model over Central Africa: Investigation of processes during the September–November rainy season. *International Journal of Climatology*, *42*(12), 6311–6331. https://doi.org/10.1002/joc.7591

Tamoffo, A. T., Vondou, D. A., Pokam, W. M., Haensler, A., Yepdo, Z. D., Fotso-Nguemo, T. C., Tchotchou, L. A. D., & Nouayou, R. (2019). Daily characteristics of Central African rainfall in the REMO model. *Theoretical and Applied Climatology*, *137*(3–4), 2351–2368. https://doi.org/10.1007/s00704-018-2745-5

Tamoffo, A. T., Weber, T., Akinsanola, A. A., & Vondou, D. A. (2023). Projected changes in extreme rainfall and temperature events and possible implications for Cameroon's socio-economic sectors. *Meteorological Applications*, *30*(2). https://doi.org/10.1002/met.2119

Wainwright, C. M., Finney, D. L., Kilavi, M., Black, E., & Marsham, J. H. (2020). Extreme rainfall in East Africa, October 2019–January 2020 and context under future climate change. *Weather*, *76*(1), 26–31. https://doi.org/10.1002/wea.3824

https://doi.org/10.5194/egusphere-2024-1257
Preprint. Discussion started: 6 May 2024

Wang, L., & Li, T. (2020). Effect of vertical moist static energy advection on MJO eastward propagation: Sensitivity to analysis domain. *Climate Dynamics*, *54*(3–4), 2029–2039. https://doi.org/10.1007/s00382-019-05101-8

Wang, T., & Li, T. (2020). Diagnosing the column-integrated moist static energy budget associated with the northward-propagating boreal summer intraseasonal oscillation. *Climate Dynamics*, *54*(11–12), 4711–4732. https://doi.org/10.1007/s00382-020-05249-8

Wantim, M. N., Ughe, W. G., Kwah, D. C., Bah, T. C., Quinette, N., & Ayonghe, S. N. (2023). Forensic investigation of the Gouache landslide disaster, Western Region, Cameroon. *Journal of the Cameroon Academy of Sciences*, *19*(3), 223–240. https://doi.org/10.4314/jcas.v19i3.3

Washington, R., James, R., Pearce, H., Pokam, W. M., & Moufouma-Okia, W. (2013). Congo Basin rainfall climatology: Can we believe the climate models? *Philosophical Transactions of the Royal Society B: Biological Sciences*, *368*(1625), 20120296. https://doi.org/10.1098/rstb.2012.0296

Wen, N., Liu, S., & Li, L. Z. X. (2022). Diagnosing the dynamic and thermodynamic effects for the exceptional 2020 summer rainy season in the Yangtze River Valley. *Journal of Meteorological Research*, *36*(1), 26–36. https://doi.org/10.1007/s13351-022-1126-2

Yanai, M., & Tomita, T. (1998). Seasonal and interannual variability of atmospheric heat sources and moisture sinks as determined from NCEP–NCAR reanalysis. *Journal of Climate*, *11*(3), 463–482. https://doi.org/10.1175/1520-0442(1998)011<0463:saivoa>2.0.co;2

https://doi.org/10.5194/egusphere-2024-1257
Preprint. Discussion started: 6 May 2024

Zhao, D., Zhang, L., & Zhou, T. (2022). Detectable anthropogenic forcing on the long-term changes of summer precipitation over the Tibetan Plateau. *Climate Dynamics*, *59*(7–8), 1939–1952. https://doi.org/10.1007/s00382-022-06189-1

Zhou, L., Tian, Y., Myneni, R. B., Ciais, P., Saatchi, S., Liu, Y. Y., Piao, S., Chen, H., Vermote, E. F., Song, C., & Hwang, T. (2014). Widespread decline of Congo rainforest greenness in the past decade. *Nature*, *509*(7498), 86–90. https://doi.org/10.1038/nature13265